Mechanistic models of humoral kinetics following COVID-19 vaccination

Daniel Stocks MEng[1*], Dr Amy Thomas BSc, PhD[2†],
Prof Adam Finn MA, BM, BCh, PhD[2], Dr Leon Danon MSci,
MSc, PhD[1†], Prof Ellen Brooks-Pollock MSci, PhD[2†]

[1]School of Engineering Mathematics and Technology, University of Bristol, Tankard's Close, Bristol, BS8 1TW, United Kingdom.
[2]Population Health Sciences, Bristol Medical School, University of Bristol, Oakfield Grove, Bristol, BS8 2BN, United Kingdom.

*Corresponding author(s). E-mail(s): ds17060@bristol.ac.uk;
Contributing authors: amy.thomas@bristol.ac.uk;
Adam.Finn@bristol.ac.uk; l.danon@bristol.ac.uk;
ellen.brooks-pollock@bristol.ac.uk;
[†]These authors contributed equally to this work.

Abstract

Introduction: Future COVID-19 vaccine programmes need to take into account the variable responses elicited by different vaccines and their waning protection over time. Existing descriptions of antibody response to COVID-19 vaccination convey limited information about the mechanisms of antibody production and maintenance.

Methods: We describe the antibody dynamics elicited by COVID-19 vaccination with two biologically-motivated mathematical models of antibody production by plasma cells and subsequent decay. We fit the models using Markov Chain Monte Carlo to seroprevalence data from 14,602 uninfected individuals collected via the primary care network in England between May 2020 and September 2022. We ensure our models are structurally and practically identifiable when using antibody data alone. We analyse the effect of age, vaccine type, number of doses, and the interval between doses on antibody production and longevity of response.

Results: We find evidence that individuals over 35 years of age who received a second dose of ChAdOx1-S generate a persistent antibody response suggestive

1

of long-lived plasma cell induction, while individuals that receive two doses of BNT162b2, or one dose of either vaccine do not. We also find that plasamblast productive capacity, the likely driver of short-term antibody responses, is greater in younger people than older people ($\leq$ 4.5 fold change in point estimates), people vaccinated with two doses than people vaccinated with one dose ($\leq$ 12 fold change), and people vaccinated with BNT162b2 than people vaccinated with ChAdOx1-S ($\leq$ 440 fold change). The effect of age on antibody dynamics is more pronounced in people vaccinated with BNT162b2 than people vaccinated with ChAdOx1-S. We find the half-life of an antibody to be between 23 – 106 days.

Conclusion: Routinely-collected seroprevalence data are a valuable source of information for characterising within-host mechanisms of antibody production and persistence. Extended sampling and linking seroprevalence data to outcomes would allow for powerful conclusions about how humoral kinetics protect against disease.

Keywords: Within-host Model, SARS-CoV-2, Vaccination, Antibody Response, Short- and Long-lived Plasma Cell Kinetics

Introduction

Vaccination against COVID-19 is now routinely used to maintain levels of population immunity. It is important to understand how the immune response elicited by vaccination will change with time. The antibody response to vaccination varies with age ([1]; [2]; [3]; [4]), peaking within a couple of weeks and subsequently waning over the course of six months ([4]; [5]; [6]). The mRNA Pfizer-BioNTech vaccine (BNT162b2) elicits a stronger antibody response than the adenoviral vector AstraZeneca vaccine (ChAdOx1-S) after the first dose and up to two weeks after the second dose ([7]), with the response to the second dose being more than an order of magnitude greater than the response to the first dose ([7]; [8]; [9]; [10]).

Mathematical models can be used to help understand underlying mechanisms of the response, explain differences between age and vaccines, and predict future antibody levels. Previous modelling of SARS-CoV-2 specific antibody levels used statistical, single-phase exponential decay models often implemented through linear regressions ([11]; [12]; [13]; [14]; [15]; [16]). These models convey limited mechanistic information because they are not biologically motivated and are constrained by the inherent assumptions in their structure.

Analysis of the immune response is challenging because there are many unobserved components. Quantification of serum antibody concentrations offers a viable window into the dynamics of the humoral system ([17]; [18]; [19]). Serum antibody concentrations can be quantified by taking blood samples, and mucosal antibodies can be quantified in saliva or other mucosal samples, while plasma cells that reside in the bone marrow ([20]; [21]; [22]; [23]) and their precursors, B cells, that differentiate in lymph nodes are much harder to accurately quantify without invasive procedures. It is therefore of interest to see whether information about the underlying kinetics of antibody production can be extracted from data on antibody level alone.

2

Binding antibody titers have been correlated with COVID-19 vaccine efficacy (24; 25), suggesting antibody titers are important for preventing the development of serious disease and reinfection (26). Similarly, antibody levels on admission to hospital are inversely correlated with in-hospital mortality (27).

Maintenance of a persistent immune response

Biological mechanisms that maintain the humoral response after exposure (natural infection or vaccination) have been investigated (28). However, hypotheses that persisting antibody levels are a result of memory B cells being continuously stimulated through chronic infection, re-exposure, persistent antigen, or bystander T cells are not consistent with observations. The re-exposure and bystander T cell hypotheses (28) rely on pathogens being endemic and therefore cannot explain persisting antibodies in the absence of local outbreaks (29; 30; 31). The persistent antigen hypothesis is based on evidence that follicular dendritic cells (FDCs) sequester antigen in later stages of infection and, over time, display it to memory B cells to encourage a continued humoral immune response in the absence of infection (32; 33; 34). However, the decay of antigen retained by FDCs in mice is too fast to explain stable antibody production (35) although, persistent antigen could be important early in the memory response.

Other hypotheses explain persistent antibody levels with independently regulated plasma cells, instead of memory B cells. It has been shown that plasma cell populations and antibody levels persist in the absence of memory B cells (29; 36; 37; 38; 39; 40). One hypothesis that links plasma cell populations to antibody levels is competition between newly produced plasmablasts and residing, long-lived plasma cells for niches in the bone marrow (20; 21; 22; 23; 41). However, this hypothesis predicts a faster decline in long-term antibody levels in older people, which is not observed (29). A different hypothesis (the '*imprinted lifespan*' hypothesis) proposed in (28) is that plasma cells are imprinted with a short or a long lifespan upon differentiation from B cells. B cells that differentiate without interaction with CD4$^+$ T cells (T cell independent) and are cross-linked by repetitive foreign antigen become short-lived plasma cells (plasmablasts) (28). Whereas, a lifespan of years or decades is thought to be achieved by B cells that are cross-linked by a non-repetitive foreign antigen and interact with CD4$^+$ T cell (T cell dependent) (28). To acquire even longer lifespans (potentially as long as the person themselves) B cells must be cross-linked by repetitive foreign antigen and interact with CD4$^+$ T cells (28).

Following a mathematical formulation of the '*imprinted lifespan*' hypothesis proposed in (18) we analyse two mathematical models. One model includes long-lived plasma cells, the other does not. Figure 1 shows a qualitative description of the modelled humoral dynamics, similar to those observed in vivo (42). We impose the requirement that models are structurally identifiable and then ensure that they are practically identifiable, i.e. that observed outputs can only be generated by a single parameter set (a different parameter set would generate a different output) (43; 44; 45), and that the data contain enough information to inform the parameters.

We assess parameter identifiability to understand which model describes the kinetics of the humoral response after one and two doses of COVID-19 vaccination
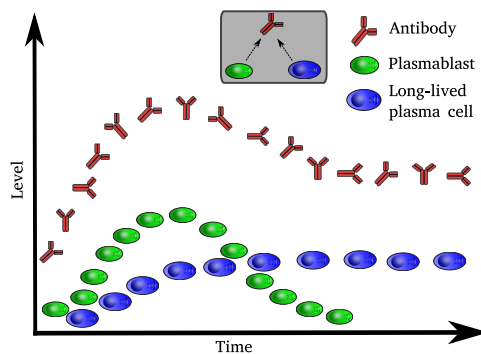
3

Fig. 1 A schematic of modelled humoral dynamics. A persistent antibody response is dependent on the generation of long-lived plasma cells. In contrast, early antibody dynamics and peak serum antibody concentrations are driven by short-lived plasma cells (plasmablasts).

for different ages and vaccine schedules. From our analysis, we draw conclusions on which groups show evidence of long-term antibody responses, how age and vaccine schedule impact antibody levels, and the importance of a second dose.

Results

Antibody dynamics by age and vaccine type

We split the data on antibody level into age groups (16 – 34, 35 – 54, 55 – 74, 75+), vaccine type (BNT162b2, ChAdOx1-S), and number of doses (one or two), prior to model fitting. Using two models of antibody dynamics, derived from biologically motivated equations of humoral kinetics (equation (2) and equation (3)), we are able to describe the SARS-CoV-2 specific antibody response of 7 of the 8 first dose groups and 8 of the 16 second dose groups, and make predictions about future antibody levels. Table 2 contains the groups we are able to model. A group can be modeled if using

its data, all the parameters of one of the models are identifiable (i.e. the model is identifiable).

The antibody dynamics of all modelled first dose groups can be described by the single cell model, while the asymptotic model only describes 35 – 54 year-olds vaccinated with one dose of BNT162b2. However, the single cell model is a better predictor of the data collected from this group than the asymptotic model. Bayes' Factor is 159,000 for the single cell model over the asymptotic model.

We are able to model seven of the second dose groups (see table 2). The antibody dynamics of 35 – 54 year-olds and 55 – 74 year-olds, and 75+ year-olds vaccinated with two doses of ChAdOx1-S is better described (measured by Bayes' Factor) or can only be described by the asymptotic model. Data collected from 55 — 74 year-olds who received two doses of ChAdOx1-S greater than 77 days apart were better predicted by the asymptotic model, with a Bayes' Factor of 63.0 for the asymptotic model over the single cell model. The antibody dynamics of 75+ year-olds vaccinated with two doses of BNT162b2 can only be described by the single cell model. Data collected from 16 — 34 year-olds who received two doses of BNT162b2 at most 77 days apart was better predicted by the asymptotic model, with a Bayes' Factor of 12.1 for the asymptotic model over the single cell model.

Figure 2 shows the dynamics of the modelled groups given in table 2. For the first dose the models are initialised at zero ($A_0 = 0$). It is assumed in the asymptotic and single cell models that the initial population of plasma cells is the full population that then decays. This assumption results in an immediate sharp

4

rise in antibody levels. This sharp rise does not reflect what we observe in the data for the antibody response to the first dose but does for the response to the second dose.

Age has a greater impact on the magnitude of the antibody response for people vaccinated with BNT162b2 than those vaccinated with ChAdOx1-S. After both the first and second dose, younger people vaccinated with BNT162b2 have higher antibody levels than older people vaccinated with BNT162b2 at all time points and our models predict this trend will continue into the future. While for those vaccinated with ChAdOx1-S there is little discrepancy between the age groups, especially after the second dose.

We also find that those vaccinated with one dose of BNT162b2 have higher antibody levels than the same age group vaccinated with one dose of ChAdOx1-S in the short-term but lower levels in the long-term. The length of time those vaccinated with BNT162b2 have higher antibody levels than the same age group vaccinated one dose of ChAdOx1-S is age dependent. Younger people vaccinated BNT162b2 have higher antibody levels than the same age group vaccinated with ChAdOx1-S for longer than older people. The time of cross-over is 113.4 days, 90.0 days, and 33.4 days, for 34 – 35 year-olds, 55 – 74 year-olds, and 75+ year-olds, respectively. However, the 95% HPD CrIs of the means overlap for the whole time-frame of the first dose data (215 days post vaccination), so we cannot say with confidence that a cross-over occurs in the timeframe of these data. We do not have a comparison for 16 – 34 year-olds because the data on this age group's response to one dose of ChAdOx1-S were insufficient to identify a model.

We also find that people vaccinated with two doses of BNT162b2 will have higher antibody levels than those vaccinated with ChAdOx1-S for approximately nine months after receiving their second dose. However, our models predict that after nine months the levels will be similar and in the long-term, those vaccinated with ChAdOx1-S will have higher antibody levels. A possible exception is 16 – 34 year-olds vaccinated with BNT162b2. This group is best described by the asymptotic model. However, the 95% HDP CrI for the group's antibody dynamics includes decaying to zero in the long-term. So, we cannot be confident 16 – 34 year-olds vaccinated with two doses of BNT162b2 will have persisting antibodies. This wide interval is probably due to the small sample size of the group ($n = 25$).

Estimates of Humoral Response Parameters

Even though only 14 of the 24 groups we investigate can identify all the parameters of at least one of the proposed models and are therefore the only groups we can say the models describe, we can still extract information about individual, identifiable parameters from all groups. Figure 3 shows the mode and 95% HPD CrI of the posterior distribution of parameters for groups whose data are able to identify them.

A common pattern for both models after both doses is that the value of Φ_s (the antibody production capacity of short-lived plasma cells) decreases with age and is greater for those who received BNT162b2 than those who received ChAdOx1-S. This result explains the higher peak antibody response after vaccination in younger people and people vaccinated BNT162b2 observed in figure 2. Similarly, comparing the estimates of Φ_s between the first and second
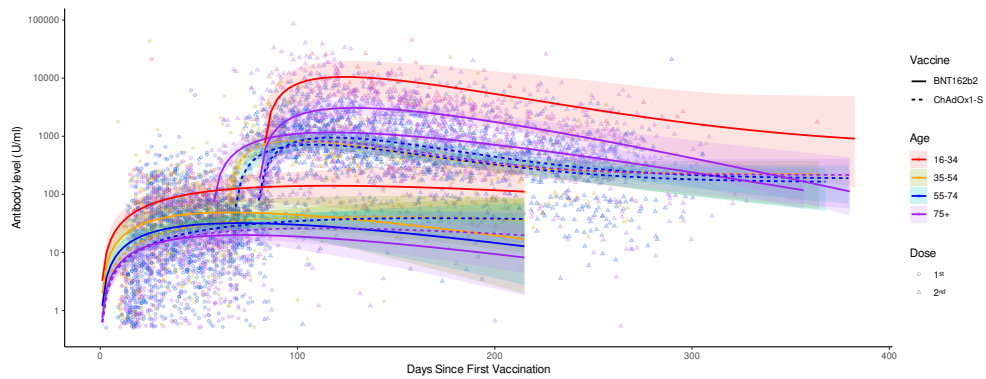
5

Fig. 2 The antibody data and best fitting model of the group whose data could identify a model (the groups in table 2). The models for people who have received two doses ChAdOx1-S are the asymptotic model, and all others models are the single cell model. For the first dose we initialise the models at zero ($A_0 = 0$). All parameter estimates are given in table 2. The shaded regions are defined by the 95% HPD CrI of the parameter estimates.

doses, we see that both models estimate an increase of 10- to 100- and 70- to 440-fold in Φ_s when people receive their second dose of ChAdOx1-S and BNT162b2, respectively. These increases explain the higher peaks after two doses observed in figure 2.

A weak distinction between the group estimates of μ_s and μ_a (short-lived plasma cell decay rate and antibody decay rate respectively) in the first dose groups is found by both models. The model fitting suggests people 35 and older who received BNT162b2 have faster rates of plasma cell and antibody decay than those who received ChAdOx1-S. This explains why people vaccinated with one dose of ChAdOx1-S maintain a high antibody level than the same age group who received one dose of BNT162b2, observed in figure 2. However, this pattern is not found after the second dose.

For there to be evidence of a long-term antibody response in a group Φ_l (the antibody production capacity of long-lived plasma cells) must be greater than zero. Only people 35 and older who received

two doses of ChAdOx1-S were found to show strong evidence of a long-term antibody response. For 35-54 year-olds this is only true if they received their doses more than 77 days apart and for people 75 and older this is only true if they received their doses less than 77 days apart. The data collected from 16 – 34 years-olds and 35 – 54 year-olds vaccinated with one BNT162b2, and 16 – 34 years-olds vaccinated with two doses of BNT162b2 was able to identify Φ_l, suggesting these groups could have mounted a long-lived immune response. However, the 95% HDP CrI are [0–5.24], [0–2.23], [0–59.4], and [0–40.6] respectively, all include zero and therefore we cannot be confident long-lived plasma are induced.

Taken together these observations provide quantifiable explanations for observed difference in antibody dynamics between vaccine types and age groups. They show that we only find evidence of a persisting antibody response and thus likely induction of long-lived plasma cells in people vaccinated with two doses of ChAdOx1-S. They also explain

6

greater peak antibody response observed in younger people than older people, people who receive one dose than people who receive two, and people vaccinated with BNT162b2 than people vaccinated with ChAdOx1-S, by more productive short-lived plasma cell (plasmablast) populations.

Methods and Materials

Antibody Data

We use SARS-CoV-2 specific antibody data collected from 355,019 routine blood tests between May 2020 and September 2022 collected and validated by the Oxford-Royal College of General Practitioners (RCGP) (see figure 2) (46). This dataset contains vaccination dates and level of total antibody (sum of IgG, IgA, IgM) against the SARS-CoV-2 receptor binding domain (RBD) on the spike (S) protein, measured in units per milliliter (U/ml) at various times after one, two, three or four doses. Due to the sparsity of data after three and four doses, we only use the data after one and two doses.

Previous infection with SARS-CoV-2 can be distinguished from vaccination by seeing whether an individual's antibodies bind to nucleocapsid (N) protein as well as spike (S) protein. This has been recorded in the data alongside an individual's vaccine type, number of doses, interval between doses, and age. These factors are used to stratify the population into groups. We assume that the antibody dynamics of the people within a group are the same, therefore individuals' one-off samples can be interpreted as longitudinal data for the group. As we are investigating the effects of vaccination on antibody levels, we remove anyone who has evidence of previous infection

i.e., antibodies that bind to N protein (N positive).

Individuals are categorised by age: 16 – 34 years, 35 – 54 years, 55 – 74 years and 75+ years. We included the BNT162b2 and ChAdOx1-S vaccines and one and two doses and whether the doses were administered less than or equal to 77 days apart or more than 77 days apart (two dose intervals used in the United Kingdom). As we have set four age categories, two vaccine categories, and two dose interval categories, there are 8 possible groups for the first dose and 32 possible groups for the second dose. We have adequate data (i.e. as many time points as parameters for our largest model) for all first dose groups but only 16 of the second dose groups. We do not have adequate data for people who were heterologously vaccinated.

Mathematical Models

The general model proposed in (18) is the 'complete' exponential model, that captures the kinetics of short-lived plasma cells P_s, long-lived plasma cells P_l, and antibodies A:

$$\frac{dP_s}{dt} = -\mu_s P_s, \tag{1a}$$

$$\frac{dP_l}{dt} = -\mu_l P_l, \tag{1b}$$

$$\frac{dA}{dt} = \phi_s P_s + \phi_l P_l - \mu_a A, \tag{1c}$$

where μ_s, μ_l and μ_a denote the decay rate of short-lived plasma cells, long-lived plasma cells, and antibodies respectively, and ϕ_s and ϕ_l denote the rate short- and long-lived plasma cells secretes antibodies, respectively. However, it was found in (18) that assuming $\mu_l = 0$ best describes longitudinal data on hepatitis A specific antibodies with samples taken up to 114 months after vaccination. Hence,
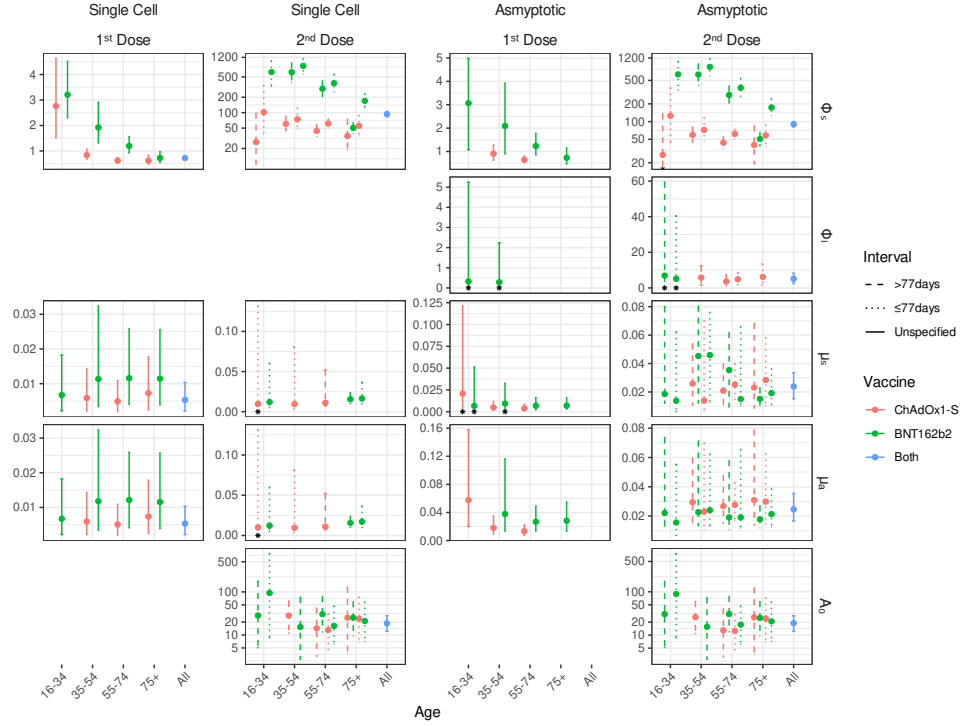
7

Fig. 3 The mode and 95% HDP CrI of the parameter's posterior distribution for both doses and models, when the parameter is identifiable. The line type is used to distinguish between dosing interval, with dashed and dotted lines used for people who received their second dose > 77 days or ≤ 77 days after their first dose respectively, and solid lines are used for groups without a specified dose interval. A dose interval is not specified for first dose groups and when we do not split the data for the dose. Colours are used distinguish between the vaccines. For the second dose only one vaccine is specified for the groups because we only have adequate data for homologously vaccinated people (e.g. someone who received ChAdOx1-S for their second dose also received it for their first dose). Red is used for ChAdOx1-S, green for BNT162b2, and blue for when we do not split the data by vaccine brand. Blue points with blue solid error bars represent the estimates and 95% HDP CrI of parameters fit to all the data on that dose. The black asterisks mark when the lower bound of the parameters 95% HDP CrI is zero.

we set $\mu_l = 0$, implicitly assuming long-lived plasma cells live forever, and solve the system of equations (1) with the initial conditions $P_s(0) = P_s^0$, $P_l(0) = P_l^0$, and $A(0) = A_0$ to obtain,

$$A(t) = \frac{\Phi_l}{\mu_a} + \frac{\Phi_s}{\mu_a - \mu_s}e^{-\mu_s t}$$
$$+ \left(A_0 - \frac{\Phi_l}{\mu_a} - \frac{\Phi_s}{\mu_a - \mu_s}\right)e^{-\mu_a t}, \quad (2)$$

where $\Phi_s = \phi_s P_s^0$ and $\Phi_l = \phi_l P_l^0$. The new parameters Φ_s and Φ_l represent the maximum antibody production of the respective plasma cells populations and are defined so that equation (2) is structurally identifiable. We will refer to Φ_s and Φ_l as the productive capacity of short-live and long-lived plasma cells, respectively.

8

We also consider a related model (the single cell model) that assumes long-lived plasma cells are not induced ($\Phi_l = 0$).

$$A(t) = \frac{\Phi_s}{\mu_a - \mu_s}\left(e^{-\mu_s t} - e^{-\mu_a t}\right) + A_0 e^{-\mu_a t}. \quad (3)$$

Model Fitting

We use a Bayesian framework to fit our models (equation (2) and equation (3)) to the data, implemented in R with the rstan package (available at: https://mc-stan.org/). A Markov Chain Monte Carlo (MCMC) algorithm is used to estimate the joint posterior distribution of the parameters.

To obtain a likelihood function we assume that the log of the antibody levels can be modelled as a random variable, $X(t)$, drawn from a normal distribution with a mean defined our model, $A(t,\theta)$, and a standard deviation σ.

$$X(t) \sim \mathcal{N}\big(A(t,\theta), \sigma\big),$$
$$P(X(t) = x|\theta) = \frac{1}{\sigma\sqrt{2\pi}} e^{-\frac{(x - A(t,\theta))^2}{2\sigma^2}}.$$

Initial conditions and prior distributions

When modelling the first dose response we set the initial antibody level, A_0, to zero (as we assume people have not been exposed to SARS-CoV-2) and for the response to the second dose we assume A_0 is log-normally distributed with mean μ_{A_0} and standard deviation σ_{A_0}. The values of μ_{A_0} and σ_{A_0} are estimated from the antibody levels of people recorded after their first dose. As the data are cross-sectional, we cannot know what each individual's antibody level was when they were given their second dose. Hence, we sample the log-transformed serum antibody concentrations after the first dose on the days when the people recorded after their second dose were vaccinated. The mean and standard deviation of this normally distributed sample are used as μ_{A_0} and σ_{A_0} respectively.

For the decay parameters, μ_s and μ_a, we use the same log-normal prior for both. A log-normal prior is used because we expect the values of μ_s and μ_a to be small (30; 36; 47; 48; 49; 50; 51; 52; 53), but greater than zero. We calibrate the prior by setting its 2.5% and 97.5% quantiles to 0.01 and 0.1 respectively (equivalent to assuming there is a 95% probability that the true parameter value lies between these values). This reflects the belief that the expected half-lives of antibodies and short-lived plasma cells are in the tens of days (30; 36; 47; 48; 49; 50; 51; 52; 53).

The production capacity parameters, Φ_s and Φ_l are more difficult to inform from literature as they are artificial. However, Φ_l can still be informed through assumptions about the long-term dynamics of the model. The resting antibody level at t_∞ is predicted by the asymptotic model (equation 2) to be $\frac{\Phi_l}{\mu_a}$, so Φ_l will be equal to the product of μ_a and the resting antibody level, which we denote lAb_∞. We have assumed that both the antibody data and μ_a are log-normally distributed. The product of two log-normal distributions is log-normally distributed. If we say the mean and standard deviation of the prior for μ_a is μ_{decay} and σ_{decay} respectively, and the mean and standard deviation of the resting antibody level is μ_∞ and σ_∞ respectively, the prior for Φ_l will have the mean and standard deviation $\mu_{\Phi_l} = \mu_{\text{decay}} + \mu_\infty$ and $\sigma_{\Phi_l} = \sigma_{\text{decay}}^2 + \sigma_\infty^2 - 2\sigma_{\text{decay}}\sigma_\infty$. We calculate μ_∞ and σ_∞ through assuming

the 2.5% and 97.5% quantiles of the distribution. After the first dose we assume the 2.5% and 97.5% quantiles of the log-transformed resting antibody level will be 2 and 7 respectively and after the second dose the 3 and 8, respectively. These quantiles are informed by the data we have on earlier time points, therefore not violating the principle of prior belief being ignorant to data, as we do not have data for long-time.

The final parameter is the production capacity of short-lived plasma cells, Φ_s. There is not the same intuitive interpretation for Φ_s in the dynamics of the model as there is for Φ_l so we use a truncated normal distribution with the 2.5% and 97.5% quantiles 1 and 5 respectively for the first dose and 50 to 1000 respectively for the second dose. These quantiles were calibrated through prior predictive checks.

To summarise, the prior distributions are,

$$\Phi_s \sim Truncnormal(\mu_{\Phi_s}, \sigma_{\Phi_s}), \quad (4a)$$

$$\Phi_l \sim Lognormal(\mu_{\Phi_l}, \sigma_{\Phi_l}), \quad (4b)$$

$$\mu_s \sim Lognormal(\mu_{\text{decay}}, \sigma_{\text{decay}}), \quad (4c)$$

$$\mu_a \sim Lognormal(\mu_{\text{decay}}, \sigma_{\text{decay}}), \quad (4d)$$

$$A_0 \sim Lognormal(\mu_{A_0}, \sigma_{A_0}). \quad (4e)$$

Parameter Identifiability

We use the STRIKE GOLDD Matlab package (54) (available at https://github.com/afvillaverde/strike-goldd) to determine whether our models are structurally identifiable. We use STRIKE GOLDD because it considers initial condition as parameters and has tools for reparameterization in the case of structural non-identifiability.

The true value of a structural identifiable parameter is theoretically possible to find, given noise-free data. It may not be possible to determine the true value of a structurally identifiable parameter when fitting to noisy or sparse data. Practical identifiability, defined as the ability to define finite bounds around an estimate (55), determines whether the data contain enough information to estimate the parameter value with confidence.

An established method of defining confidence intervals is with the profile likelihood method (55), by assuming values of the parameter and maximising the likelihood function with respect to the remaining parameters (the 'nuisance' parameters) (55; 56; 57). The simplest implementation of maximisation uses maximum likelihood estimation (MLE) and gradient decent methods (55; 57). Though the methodology of the profile likelihood method is well defined it can be fragile when likelihood spaces are complex and difficult to navigate by gradient decent.

To mitigate the fragility of the likelihood profile method we use a Monte Carlo Markov Chain (MCMC) algorithm to explore the parameter space more completely and generate posterior distributions of parameter values. We determine a parameter to be practically identifiable if the 95% highest posterior density credible interval (HPD CrI) of the posterior distribution is constrained to a single biologically meaningful set and is not sensitive to prior assumptions. We say the parameter is not identifiable when the 95% HPD CrI is made up of multiple separate regions because this implies the data do not contain enough information to constrain the parameter estimate around the true value. Similarly, if the 95% HPD CrI is sensitive to prior assumptions this implies the data do not contain enough information to inform the parameter.

10

Sensitivity analysis

We conduct the sensitivity analysis by expanding the quantiles of the prior distributions of Φ_s, μ_s, μ_a, lAb$_\infty$, and doubling the standard deviation calculated for a particular group, shown in table 1. To determine whether a 95% HPD CrI is sensitive to the priors we check two things: whether the inclusion of zero in the HPD CrI has changed, and whether the modes of both posteriors are included within the HPD CrI of both posteriors. If the inclusion of zero in HPD CrI changes, so does the conclusion about whether the effect of the parameter can be detected in the data. This is a fundamental change, and we say the posteriors are too sensitive to the prior in this case. Checking if the modes of the posteriors are included within the HPD CrI of the other posterior is to test for agreement in the estimates. If there is agreement, we say the posterior is not too sensitive to the priors.

Discussion

We have proposed and analysed two mechanistic and identifiable models of SARS-CoV-2 specific antibody dynamics that link cross-sectional seroprevalence data to within-host antibody dynamics. Our models relate peak antibody levels to productive capacity of short-lived plasma cells, explaining the observation that individuals who received BNT162b2 have higher peak levels than those that received ChAdOx1-S (7), as well as a higher peak observed in younger people than older people (4; 1; 2; 3). Persistent antibody levels observed in people who receive two doses of ChAdOx1-S are presumed to be explained by the induction of long-lived plasma cells. We found no effect of age on the apparent production capacity of long-lived plasma cells.

The inability of mRNA COVID-19 vaccines to elicit long-lived plasma cells after one and two doses has been discussed previously (58). However, long-lived plasma cells in bone marrow, and improved immunogenicity, have been found in people vaccinated with three and four doses of mRNA COVID-19 vaccines (59; 60), although this may be due to infection.

Previous mathematical models of SARS-CoV-2 antibody responses were phenomenologically rather than biologically motivated, often due to data limitations (11; 12; 13; 14; 15; 16). These models considered a constant rate of antibody decay and do not account for the production of antibodies by plasma cells. Therefore, they cannot inform on the mechanisms of antibody maintenance and have limited power to predict future antibody levels. Our single cell and asymptotic models consider two and three timeframes respectively, allowing them to distinguish separate phases of decay naturally. When models only consider a single phase of decay (11; 12; 13; 14; 15; 16) model calibration is forced to compromise between short-term forces (short-lived plasma cells, antibody decay) and long-term forces (long-lived plasma cells), so parameter estimates and predicted dynamics can be difficult to interpret.

Previous modelling estimated the half-life of antibodies to be hundreds of days (11; 12; 13) with wide confidence intervals (11). In contrast, our model explicitly captures the kinetics of antibody production and our point estimates of the half-life of antibodies (23 – 116 days) are consistent with experimental findings (47; 49; 50; 51; 52; 36) and previous estimates (15; 16). Our improved estimates are due to our approach's ability to overcome the restrictions of single-phase

Table 1 Prior distributions for the model parameters. For Φ_s, μ_s, μ_a, and lAb_∞ we assume the 2.5% and 97.5% quantiles of the prior distributions. For A_0 the assumptions are the mean and standard deviation. Values are not given for the A_0 assumptions as they vary between the groups.

Dose	Baseline Prior Assumptions				
	Φ_s	μ_s	μ_a	lAb_∞	A_0
1st	[1, 5]	[0.01, 0.1]	[0.01, 0.1]	[2, 7]	-
2nd	[50, 1000]	[0.01, 0.1]	[0.01, 0.1]	[3, 8]	μ_{A_0}, σ_{A_0}
Dose	Sensitivity Analysis Prior Assumptions				
	Φ_s	μ_s	μ_a	lAb_∞	A_0
1st	[0.5, 10]	[0.005, 0.1]	[0.005, 0.1]	[1, 8]	-
2nd	[50, 2000]	[0.005, 0.1]	[0.005, 0.1]	[2, 9]	μ_{A_0}, $2\sigma_{A_0}$

models with a description of antibody dynamics that considers their production. Single-phase models overestimate the half-life of antibodies to compensate for the lack of antibody renewal. Half-life estimates of from single-phase models can depend on how many doses a person received (16). The change in estimates following booster doses will likely be due to the effects of memory B cells that become dominant in the humoral response, and the induction of long-lived plasma cells, effects our model captures and overcomes.

A limitation of our models is the assumption that the initial population of plasma cells is the full population that decays over time. In actuality, after vaccination, antigen will be produced within the host's cells (61), presented to naive and memory B cells within the lymph nodes by follicular dendritic cells, which then through various routes proliferate and differentiate into plasma cells (62). A more accurate model could include the initial expansion of the plasma cell population. Such a model would fit the initial antibody response better and give information on differences in plasma cell generation post vaccination between population groups. The improved fitting would be most pronounced for responses to the first dose as that is when we would not

expect people to have SARS-CoV-2 specific plasma cells prior to vaccination. However, such a model would require data of other immune factors such as germinal center B cells, which are not easy to obtain. Another limitation is the length of time over which the data were collected. Data that continued further after each dose would help clarify long-time dynamics and help validate our predictions. Due to identifiability issues, it is not possible for our models to distinguish the plasma cell number and rate of antibody production from each other. So, we cannot determine what combination of these two factors is responsible for variation in the overall production of antibodies between groups.

Our models suggest that while mRNA vaccines induce larger short term responses which may have advantages for rapid protection, the adenoviral vector vaccines may have advantages in eliciting persistent serum antibodies against SARS-CoV-2, presumably through induction of long-lived plasma cells. Vaccinating people who have only received mRNA vaccines with adenoviral vector vaccines, with priority given to older people, may achieve persistently high antibodies in all age groups. Clinical studies into the effectiveness of BNT162b2 and ChAdOx1-S against infection with

SARS-CoV-2 and hospitalisation with COVID-19 find that BNT162b2 and ChAdOx1-S are comparable after one dose, but BNT162b2 is more effective after two doses (63; 64; 65; 66; 67; 68; 69). However, comparisons of BNT162b2 and ChAdOx1-S vaccine effectiveness are usually short term, at most up to 30 weeks, whereas our models cover longer timescales. Further, we cannot be certain whether heterologous vaccination will elicit the same humoral response and effectiveness as homologous vaccination. Clinical studies have found that heterologous vaccination is more effective than homologous vaccination at protecting against infection (70; 71; 72; 73). However, these findings are for adenoviral vector-primed mRNA-boosted individuals while we are discussing boosting mRNA-primed individuals with adenoviral vector vaccine. It has been found that binding and neutralizing antibodies wane less in individuals primed with mRNA vaccine and boosted with adenoviral vaccine than in individuals vaccinated with other heterologous vaccination regimes (74; 75), supporting mRNA priming and adenoviral vector boosting to achieve persistently high antibody levels.

Conclusion

Routinely-collected seroprevalence data are valuable for characterising within-host mechanisms of antibody production and persistence. Extended sampling and linking seroprevalence data to outcomes would allow for powerful conclusions on the relationship between humoral kinetics and protection against disease. With added data on other immune factors, such as serum memory B cell and plasmablasts, mathematical modelling can give more accurate descriptions of the complex kinetics of the humoral response. Closer interaction between mathematical modelers and immunologists on data collection and model structure will equip interdisciplinary groups with the necessary information to describe population immune responses more accurately, benefiting the fields of immunology and epidemiology. With the current data we can make projections of antibody responses into the future and our results suggest older people who have not received adenoviral vector vaccine may derive longer lasting protection from a booster dose of this vaccine type than from additional mRNA vaccination.

Data availability

The United Kingdom Health and Security Agency (UKHSA) dataset can be accessed by researchers; approval is on a project-by-project basis (https://orchid.phc.ox.ac.uk/index.php/orchid-data/).

13

Competing interests

The authors declare no competing interests.

References

[1] Weisberg, S. P. *et al.* Distinct antibody responses to SARS-CoV-2 in children and adults across the COVID-19 clinical spectrum. *Nature Immunology* **22**, 25—31 (2021).

[2] Dowell, A. C. *et al.* Children develop robust and sustained cross-reactive spike-specific immune responses to SARS-CoV-2 infection. *Nature Immunology* **23**, 40—49 (2022).

[3] Collier, D. A. *et al.* Age-related immune response heterogeneity to SARS-CoV-2 vaccine BNT162b2. *Nature* **596**, 417–422 (2021).

[4] Wei, J. *et al.* Antibody responses to SARS-CoV-2 vaccines in 45,965 adults from the general population of the united kingdom. *Nature Microbiology* **6**, 1140–1149 (2021).

[5] Evans, J. P. *et al.* Neutralizing antibody responses elicited by SARS-CoV-2 mRNA vaccination wane over time and are boosted by breakthrough infection. *Science Translational Medicine* **14** (2022).

[6] Qi, H. *et al.* The humoral response and antibodies against SARS-CoV-2 infection. *Nature Immunology.* **23**, 1008–1020 (2022).

[7] Rose, R. *et al.* Humoral immune response after different SARS-CoV-2 vaccination regimens. *BMC Medicine* **20** (2022).

[8] Goel, R. R. *et al.* Distinct antibody and memory B cell responses in SARS-CoV-2 naïve and recovered individuals after mRNA vaccination *Science Immunology*, eabi6950 (2021)

[9] Geers, D. *et al.* SARS-CoV-2 variants of concern partially escape humoral but not T cell responses in COVID-19 convalescent donors and vaccine recipients. *Science Immunology* **6**, eabj1750 (2021)

[10] Becker, M. *et al.* Immune response to SARS-CoV-2 variants of concern England in vaccinated individuals. *Nature Communications* **12** (2021).

[11] Whitcombe, A. L. *et al.* Comprehensive analysis of SARS-CoV-2 antibody dynamics in New Zealand. *Clinical & Translational Immunology* **10** (2021).

[12] Dorigatti, I. *et al.* SARS-CoV-2 antibody dynamics and transmission from community-wide serological testing in the Italian municipality of Vo'. *Nature Communications* **12** (2021).

[13] Chen, Y. *et al.* Immune recall improves antibody durability and breadth to SARS-CoV-2 variants. *Science Immunology* **7** (2022).

[14] Achiron, A. *et al.* SARS-CoV-2 antibody dynamics and b-cell memory response over time in COVID-19 convalescent subjects. *Clinical Microbiology and Infection* **27**, 1349.e1–1349.e6 (2021).

[15] Lumley, S. F. *et al.* The duration, dynamics, and determinants of severe acute respiratory syndrome

coronavirus 2 (SARS-CoV-2) antibody responses in individual healthcare workers. *Clinical Infectious Diseases* **73**, e699–e709 (2021).

[16] Yorsaeng, R. *et al.* SARS-CoV-2 antibody dynamics after COVID-19 vaccination and infection: A real-world cross-sectional analysis. *Vaccines* **11**, 1184 (2023).

[17] Manz, R. A. *et al.* Maintenance of serum antibody levels. *Annual Reviews Immunology* **23**, 367–386 (2005).

[18] Andraud, M. *et al.* Living on three time scales: The dynamics of plasma cell and antibody populations illustrated for hepatitis A virus. *PLoS Computational Biology* **8**, e1002418 (2012).

[19] Fraser, C. *et al.* Modeling the long-term antibody response of a human papillomavirus (HPV) virus-like particle (VLP) type 16 prophylactic vaccine. *Vaccine* **25**, 4324–4333 (2007).

[20] Benner, R., Hijmans, W. & Haaijman, J. J. The bone marrow: the major source of serum immunoglobulins, but still a neglected site of antibody formation. *Clinical and Experimental Immunology* **46**, 1–8 (1981).

[21] Hyland, L., Sangster, M., Sealy, R. & Coleclough, C. Respiratory virus infection of mice provokes a permanent humoral immune response. *Journal of Virology* **68**, 6083–6086 (1994).

[22] Hill, S. W. Distribution of plaque-forming cells in the mouse for a protein antigen. Evidence for highly active parathymic lymph nodes following intraperitoneal injection of hen lysozyme. *Immunology* **30**, 895–906 (1976).

[23] Slifka, M. K., Matloubian, M. & Ahmed, R. Bone marrow is a major site of long-term antibody production after acute viral infection. *Journal of Virology* **69**, 1895–1902 (1995).

[24] Earle, K. A. *et al.* Evidence for antibody as a protective correlate for COVID-19 vaccines. *Vaccine* **39**, 4423–4428 (2021).

[25] Fong, Y. *et al.* Immune correlates analysis of the PREVENT-19 COVID-19 vaccine efficacy clinical trial. *Nature Communications* **14**, 331 (2023).

[26] Woolsey, C. *et al.* Establishment of an African green monkey model for COVID-19 and protection against re-infection. *Nature Immunology* **22**, 86–98 (2021).

[27] Mink, S. *et al.* Evaluation of SARS-CoV-2 antibody levels on hospital admission as a correlate of protection against mortality. *Journal of Internal Medicine* **293**, 694–703 (2023).

[28] Amanna, I. J. & Slifka, M. K. Mechanisms that determine plasma cell lifespan and the duration of humoral immunity. *Immunological Reviews* **236**, 125–138 (2010).

[29] Amanna, I. J., Carlson, N. E. & Slifka, M. K. Duration of humoral immunity to common viral and vaccine antigens. *New England Journal of Medicine* **357**, 1903–1915 (2007).

15

[30] SLIFKA, M. & AHMED, R. Long-term humoral immunity against viruses: revisiting the issue of plasma cell longevity. *Trends in Microbiology* **4**, 394–400 (1996).

[31] Slifka, M. K. Immunological memory to viral infection. *Current Opinion in Immunology* **16**, 443–450 (2004).

[32] MacLennan, I. C. M. Germinal centers. *Annual Review of Immunology* **12**, 117–139 (1994).

[33] Liu, Y.-J., Grouard, G., de Bouteiller, O. & Banchereau, J. Follicular dendritic cells and germinal centers. *International Review of Cytology* **166** 139–179 (1996).

[34] Tew, J. G., Kosco, M. H., Burton, G. F. & Szakal, A. K. Follicular dendritic cells as accessory cells. *Immunological Reviews* **117**, 185–211 (1990).

[35] Tew, J. G. & Mandel, T. E., Prolonged antigen half-life in the lymphoid follicles of specifically immunized mice. *Immunology* **37**, 69–76 (1997).

[36] Hammarlund, E. *et al.* Plasma cell survival in the absence of B cell memory. *Nature Communications* **8** (2017).

[37] Manz, R. A., Thiel, A. & Radbruch, A. Lifetime of plasma cells in the bone marrow. *Nature* **388**, 133–134 (1997).

[38] Ahuja, A., Anderson, S. M., Khalil, A. & Shlomchik, M. J. Maintenance of the plasma cell pool is independent of memory B cells. *Proceedings of the National Academy of Sciences*

105, 4802–4807 (2008).

[39] DiLillo, D. J. *et al.* Maintenance of long-lived plasma cells and serological memory despite mature and memory B cell depletion during CD20 immunotherapy in mice. *The Journal of Immunology* **180**, 361–371 (2008).

[40] Slifka, M. K., Antia, R., Whitmire, J. K. & Ahmed, R. Humoral immunity due to long-lived plasma cells. *Immunity* **8**, 363–372 (1998).

[41] Radbruch, A. *et al.* Competence and competition: the challenge of becoming a long-lived plasma cell. *Nature Reviews Immunology* **6**, 741–750 (2006).

[42] Garrido, C. *et al.* SARS-CoV-2 vaccines elicit durable immune responses in infant rhesus macaques. *Science Immunology* **6**, eabj3684 (2021).

[43] Tunali, E. & Tarn, T.-J. New results for identifiability of nonlinear systems. *IEEE Transactions on Automatic Control* **32**, 146–154 (1987).

[44] Ljung, L. & Glad, T. On global identifiability for arbitrary model parametrizations. *Automatica* **30**, 265–276 (1994).

[45] Xia, X. & Moog, C. Identifiability of nonlinear systems with application to HIV/AIDS models. *IEEE Transactions on Automatic Control* **48**, 330–336 (2003).

[46] Whitaker, H. *et al.* Sociodemographic disparities in COVID-19 seroprevalence across England in the Oxford RCGP primary care sentinel

16

network *Journal of Infection* **84**, 814–824 (2022)

[47] Morell, A., Terry, W. D. & Waldmann, T. A. Metabolic properties of IgG subclasses in man. *Journal of Clinical Investigation* **49**, 673–680 (1970).

[48] Spiegelberg, H. L. & Fishkin, B. G. The catabolism of human g immunoglobulins of different heavy chain subclasses. 3. the catabolism of heavy chain disease proteins and of fc fragments of myeloma proteins. *Clinical and Experimental Immunology* **10**, 599–607 (1972).

[49] Tam, S. H., McCarthy, S. G., Brosnan, K., Goldberg, K. M. & Scallon, B. J. Correlations between pharmacokinetics of IgG antibodies in primates vs. FcRn-transgenic mice reveal a rodent model with predictive capabilities. *mAbs* **5**, 397–405 (2013).

[50] Robbie, G. J. *et al.* A novel investigational fc-modified humanized monoclonal antibody, motavizumab-YTE, has an extended half-life in healthy adults. *Antimicrobial Agents and Chemotherapy* **57**, 6147–6153 (2013).

[51] Hopkins, R. J. *et al.* Safety and pharmacokinetic evaluation of intravenous vaccinia immune globulin in healthy volunteers. *Clinical Infectious Diseases* **39**, 759–766 (2004).

[52] Adner, N. *et al.* Pharmacokinetics of human tick-borne encephalitis virus antibody levels after injection with human tick-borne encephalitis immunoglobulin, solvent/detergent treated, FSME-BULIN s/d in healthy volunteers. *Scandinavian Journal of Infectious Diseases* **33**, 843–847 (2001).

[53] Goulet, D. R. *et al.* Toward a combinatorial approach for the prediction of IgG half-life and clearance. *Drug Metabolism and Disposition* **46**, 1900–1907 (2018).

[54] Villaverde, A. F., Barreiro, A. & Papachristodoulou, A. Structural identifiability of dynamic systems biology models. *PLOS Computational Biology* **12**, e1005153 (2016).

[55] Raue, A. *et al.* Structural and practical identifiability analysis of partially observed dynamical models by exploiting the profile likelihood. *Bioinformatics* **25**, 1923–1929 (2009).

[56] Murphy, S. A. & Vaart, A. W. V. D. On profile likelihood. *Journal of the American Statistical Association* **95**, 449–465 (2000).

[57] Meeker, W. Q. & Escobar, L. A. Teaching about approximate confidence regions based on maximum likelihood estimation. *The American Statistician* **49**, 48 (1995).

[58] Giannotta, G. & Giannotta, N. mRNA COVID-19 vaccines and long-lived plasma cells: A complicated relationship. *Vaccines* **9**, 1503 (2021).

[59] Schulz, A. R. *et al.* SARS-CoV-2 specific plasma cells acquire long-lived phenotypes in human bone marrow *EBioMedicine* **95**, (2023)

17

[60] Lustig, Y. *et al.* Superior immunogenicity and effectiveness of the third compared to the second BNT162b2 vaccine dose. *Nature Immunology* **23**, 940—946 (2022).

[61] Gebre, M. S. *et al.* Novel approaches for vaccine development. *Cell* **184**, 1589–1603 (2021).

[62] Murphy, K. & Weaver, C. Janeway's Immunobiology. 10, *Garland science* (2021)

[63] Flacco, M. E. *et al.* Interim estimates of COVID-19 vaccine effectiveness in a mass vaccination setting: data from an Italian Province. *Vaccines* **9**, 628 (2021).

[64] Bernal, J. L. *et al.* Effectiveness of the Pfizer-BioNTech and Oxford-AstraZeneca vaccines on COVID-19 related symptoms, hospital admissions, and mortality in older adults in England: test negative case-control study. *BMJ* **373**, (2021).

[65] Bernal, J. L. *et al.* Effectiveness of COVID-19 Vaccines against the B.1.617.2 (Delta) Variant. *NEJM* **385**, 585–594 (2021).

[66] Paris, C. *et al.* Effectiveness of mRNA-BNT162b2, mRNA-1273, and ChAdOx1 nCoV-19 vaccines against COVID-19 in healthcare workers: an observational study using surveillance data. *Clinical Microbiology and Infection* **27**, 1699-e5 (2021).

[67] Hyams, C. *et al.* Effectiveness of BNT162b2 and ChAdOx1 nCoV-19 COVID-19 vaccination at preventing hospitalisations in people aged at least 80 years: a test-negative, case-control study. *The Lancet Infectious Diseases* **21**, 1539–1548 (2021).

[68] Horne, E. M. *et al.* Waning effectiveness of BNT162b2 and ChAdOx1 COVID-19 vaccines over six months since second dose: OpenSAFELY cohort study using linked electronic health records. *BMJ* **378**, (2022).

[69] Xie, J. *et al.* Comparative effectiveness of the BNT162b2 and ChAdOx1 vaccines against COVID-19 in people over 50. *Nature Communications* **13**, (2022).

[70] Nordstörm, P., Ballin, M. & Nordström, A. Effectiveness of heterologous ChAdOx1 nCoV-19 and mRNA prime-boost vaccination against symptomatic COVID-19 infection in Sweden: A nationwide cohort study. *The Lancet Regional Health–Europe* **11**, (2021).

[71] Pozzetto, B. *et al.* Immunogenicity and efficacy of heterologous ChAdOx1–BNT162b2 vaccination. *Nature* **600**, 701–706 (2021).

[72] Hermossilla, E. *et al.* Comparative effectiveness and safety of homologous two-dose ChAdOx1 versus heterologous vaccination with ChAdOx1 and BNT162b2. *Nature Communications* **13**, (2022).

[73] Marra, A. R. *et al.* Effectiveness of Heterologous Coronavirus Disease 2019 (COVID-19) Vaccine Booster Dosing in Brazilian Healthcare Workers, 2021. *Clinical Infectious Diseases* **76**, e360—e366 (2022).

[74] Atmar, R. L. *et al.* Homologous and Heterologous COVID-19 Booster Vaccinations. *NEJM* **386**, 1046–1057 (2022).

[75] Tan, C. S. *et al.* Durability of Heterologous and Homologous COVID-19 Vaccine Boosts. *JAMA Network Open* **5**, e2226335 (2022).

Table 2 The vaccines schedule, age, size, best fitting model, parameter estimates and 95% HDP CrI of the groups whose data could identify a model. 'Pfz' and 'Az' are short hand for BNT162b2 and ChAdOx1-S respectively. 'SC' and 'Asym' are short hand for the single cell and asymptotic models respectively. The parameters Φ_s, Φ_l, μ_s, μ_a, and A_0 are the short-lived plasma cell productive capacity, the long-lived plasma cell productive capacity respectively. The short-lived plasma cell decay rate, the antibody decay rate, and the initial level of antibody respectively.

Vaccine 1st	2nd	Age	Dose Interval	Sample Size	Model	Parameter Estimates Φ_s	Φ_l	μ_s	μ_a	A_0
Az	-	35 – 54	-	352	SC	0.835 [0.673 – 1.07]	-	0.00588 [0.00214 – 0.0142]	0.00593 [0.00216 – 0.0143]	-
Az	-	55 – 74	-	870	SC	0.621 [0.535 – 0.738]	-	0.00490 [0.00193 – 0.0109]	0.00509 [0.00191 – 0.0109]	-
Az	-	75+	-	300	SC	0.615 [0.481 – 0.831]	-	0.00731 [0.00241 – 0.0177]	0.00737 [0.00251 – 0.0179]	-
Pfz	-	16 – 34	-	92	SC	3.20 [2.30 – 4.52]	-	0.00672 [0.00219 – 0.0182]	0.00673 [0.00219 – 0.0182]	-
Pfz	-	35 – 54	-	182	SC	1.92 [1.31 – 2.91]	-	0.0114 [0.00337 – 0.0324]	0.0118 [0.00341 – 0.0324]	-
Pfz	-	55 – 74	-	532	SC	1.20 [0.923 – 1.56]	-	0.116 [0.00409 – 0.0258]	0.0121 [0.00413 – 0.0260]	-
Pfz	-	75+	-	547	SC	0.722 [0.551 – 0.976]	-	0.0114 [0.00388 – 0.0256]	0.0116 [0.00391 – 0.0257]	-
Az	Az	35 – 54	>77days	453	Asym	59.5 [44.2 – 81.3]	5.82 [1.67 – 12.4]	0.0259 [0.0107 – 0.0539]	0.0294 [0.0147 – 0.0598]	25.8 [10.9 – 55.7]
Az	Az	55 – 74	≤77days	967	Asym	61.8 [51.5 – 74.5]	4.85 [1.96 – 8.56]	0.0252 [0.0146 – 0.0400]	0.0276 [0.0171 – 0.0429]	12.5 [4.45 – 37.7]
Az	Az	55 – 74	>77days	695	Asym	43.8 [34.9 – 55.9]	3.60 [1.20 – 7.43]	0.0209 [0.0109 – 0.0400]	0.0267 [0.0149 – 0.0479]	12.9 [3.07 – 41.1]
Az	Az	75+	≤77days	285	Asym	57.9 [37.9 – 88.3]	6.16 [1.74 – 13.5]	0.0284 [0.0102 – 0.0584]	0.0299 [0.0144 – 0.0627]	24.2 [6.79 – 73.2]
Pfz	Pfz	16 – 34	≤77days	25	Asym	632 [341 – 1060]	5.15 [0 – 40.6]	0.0138 [0.00612 – 0.0622]	0.0156 [0.00674 – 0.0553]	88.9 [8.64 – 761]
Pfz	Pfz	75+	≤77days	430	SC	170 [126 – 234]	-	0.0164 [0.0100 – 0.0366]	0.0171 [0.00992 – 0.0367]	21.1 [7.05 – 58.8]
Pfz	Pfz	75+	>77days	661	SC	50.4 [39.5 – 65.0]	-	0.0155 [0.0102 – 0.0236]	0.0156 [0.0102 – 0.0235]	25.2 [9.55 – 59.8]